Earth Planet. Sci. Lett. 668 (2025) 119545

Contents lists available at ScienceDirect

Earth and Planetary Science Letters

journal homepage: www.elsevier.com/locate/epsl

Garnet as a reliable timekeeper in Archean polymetamorphic terranes

Jonas Kaempf [a,*], Chris Clark [a], Tim E. Johnson [a], Mudlappa Jayananda [b], Martin Hand [c], Krishnan Sajeev [d]

[a] School of Earth and Planetary Sciences, Curtin University, Bentley, WA 6102, Australia
[b] National Institute of Advanced Studies, Indian Institute of Science Campus, Bangalore 560012, India
[c] Department of Earth Sciences, University of Adelaide, Adelaide, SA 5005, Australia
[d] Centre for Earth Sciences, Indian Institute of Science, Bangalore 560012, India

ARTICLE INFO

Editor: Dr A Webb

Keywords:
Archean metamorphism
Dharwar Craton
P–T–t
Lu–Hf garnet dating
Petrochronology
Phase equilibrium modelling

ABSTRACT

Reliably reconstructing the pressure–temperature–time (*P–T–t*) history of Archean polymetamorphic terranes is key to gaining insight into the tectonic processes operating on the early Earth. In this regard, garnet is arguably the most important mineral. Not only does it capture information about both the timing and the conditions of metamorphism, but can also preserve this record through multiple tectonic cycles. Here, we used in situ Lu–Hf dating of garnet from two greenstone belts in the Western Dharwar Craton (WDC) in southern India to investigate their tectono-metamorphic evolution. Garnet ages reveal a record of two distinct medium- to high-pressure tectono-metamorphic events during the Archean eon. Whereas garnet from the Holenarsipur Greenstone Belt grew during late Neoarchean metamorphism at 2.53 Ga, garnet from the Kalyadi Greenstone Belt records a 2.96 Ga regional metamorphic episode that has not previously been recognized. Coupled with results from in situ monazite U–Pb dating and thermodynamic modelling, our data suggest that the two neighboring greenstone belts, which were previously thought to share a common tectonothermal history, underwent contrasting *P–T–t* evolutions throughout the Mesoarchean and Neoarchean, challenging existing models for the tectonic evolution of the WDC. Obtaining reliable age constraints in polymetamorphic terranes via in situ Lu–Hf dating of garnet that can be directly linked to *P–T* information represents a key advance in deciphering the cryptic record of crustal metamorphism throughout Earth history.

1. Introduction

Reconstructing Earth's early (Hadean and Archean; 4.5–2.5 Ga) tectonothermal history remains a challenge due to the scarcity of direct evidence. To this aim, investigations of metamorphic rocks from Archean (4.0–2.5 Ga) cratons, the ancient cores of the continents, are key (e.g., Brown and Johnson, 2018; Kuang et al., 2023). Obtaining reliable information on the pressure–temperature–time (*P–T–t*) history of such ancient rocks is challenging as most have experienced multiple tectono-metamorphic cycles, with evidence for older tectono-metamorphic event(s) obscured or erased (Alfing et al., 2024; Cutts et al., 2024; Kaempf et al., 2024a, 2024b). Although some accessory mineral geochronometers such as zircon and monazite can retain isotopic evidence of older events (e.g., Hermann and Rubatto, 2003; Simmat and Raith, 2008), direct correlations between their age and the *P–T* information recorded by the (partially) recrystallized metamorphic assemblage in which they occur can be ambiguous, leading to contentious interpretations that have profound implications for our understanding of the geodynamic processes operating on the early Earth. For example, when eclogites appeared in the geological record is debated (Skublov et al., 2011; Volodichev et al., 2021), but is of fundamental importance to the temporal emergence of deep subduction and modern-style plate tectonics (Brown et al., 2024; Palin et al., 2020).

In situ Lu–Hf geochronology via laser ablation inductively coupled plasma tandem mass spectrometry (LA–ICP–MS/MS) (Simpson et al., 2021) provides an opportunity to directly address the timing of metamorphism using garnet, a key mineral in deciphering the *P–T–t* record of polymetamorphic rocks (Baxter et al., 2017). We apply this technique to investigate the metamorphic evolution of metapelitic rocks from the Holenarsipur Greenstone Belt (HGB) and Kalyadi Greenstone Belt (KGB) in the core of the Western Dharwar Craton (WDC), southern India. Previous work has concluded that metapelitic rocks in the HGB preserve evidence of Mesoarchean (*c.* 3.1 Ga) metamorphism in domains of low strain that escaped a widespread late Neoarchean (*c.* 2.5 Ga)

* Corresponding author.
E-mail address: jonas.kaempf@curtin.edu.au (J. Kaempf).

https://doi.org/10.1016/j.epsl.2025.119545
Received 20 September 2024; Received in revised form 29 May 2025; Accepted 16 July 2025
Available online 22 July 2025

metamorphic overprint (Dasgupta et al., 2019; Jayananda et al., 2013). However, as both metamorphic events are inferred to record nearly identical *P–T* conditions (~650 °C and 7–8 kbar; Dasgupta et al., 2019, 2022) it remains challenging to assess the extent of overprinting without direct correlation between the *P–T* and age data.

Here, through integrated thermodynamic modelling and in situ Lu–Hf garnet and U–Pb monazite dating of metasedimentary samples, we reconsider the metamorphic evolution of supracrustal rocks in the WDC and identify two temporally distinct Archean (poly)metamorphic cycles, the older of which has not previously been recognized. In constraining the temporal record of metamorphism, we illustrate the potential shortcomings of relying solely on accessory phase geochronology, and demonstrate the utility of in situ Lu–Hf dating of garnet in reconstructing the tectonothermal evolution of polymetamorphic terranes throughout Earth's history.

2. Methods and materials

The HGB and KGB constitute the northernmost extent of the oldest volcano-sedimentary greenstone sequence (the 3.4–3.2 Ga Sargur Group; Jayananda et al., 2008, 2023) in the Dharwar Craton (Fig. 1a). Supracrustal rocks crop out as NNW–SSE trending belts or enclaves within spatially-associated 3.4–3.2 Ga tonalite–trondhjemite–granodiorite (TTG) gneisses. The greenstone sequences consist of metamorphosed ultramafic to felsic volcanic rocks, pelites, sandstones, conglomerates and banded iron formations (BIFs). Widespread amphibolite-facies metamorphism across the central WDC has been constrained to *c.* 2.5 Ga (Bouhallier, 1995; Jayananda et al., 2013), and variably overprints an older Mesoarchean tectono-metamorphic event, evidence for which is only locally preserved in the HGB (Dasgupta et al., 2019; Jayananda et al., 2013). Samples for this study were collected from three different localities across the HGB and from one locality in the KGB (Fig. 1b), and contain typical Barrovian-type regional metamorphic mineral assemblages (i.e., biotite–garnet–staurolite–kyanite; Fig. 2), but notably lack white mica. Detailed petrographic descriptions of all investigated samples are given in the Supplementary Material S1 and sample locations are provided in Table S1.

In situ Lu–Hf garnet dating was undertaken on eight samples from the HGB and KGB to explore the extent of preservation of Mesoarchean metamorphism. Analytical procedures for the acquisition of Lu–Hf isotopes in garnet via LA–ICP–MS/MS closely follow those described by Simpson et al. (2021) and are further outlined in the Supplementary Material S1. Results for the Lu–Hf isotopic composition of unknowns and reference materials are given in Table S2. In situ U–Pb monazite dating and acquisition of trace elements via laser ablation split-stream (LASS) ICP–MS was undertaken on two samples from the KGB and one sample from the HGB to further explore and constrain their metamorphic age record. Analytical conditions and U–Pb isotopic and trace element compositions of monazite are given in the Supplementary Material S1 and Table S3, respectively.

Phase equilibrium modelling of representative samples from both greenstone belts was undertaken to constrain their *P–T* evolution. Isochemical phase diagrams (pseudosections) were constructed using Perple_X version 6.9.0 (Connolly, 1990, 2009, 2005) and the internally consistent thermodynamic dataset ds62 (updated February 6, 2012) of Holland and Powell (2011). Modelling was carried out in the eleven-component $MnO–NaO_2–CaO–K_2O–FeO–MgO–Al_2O_3–SiO_2–H_2O–TiO_2–O_2$ (MnNCKFMASHTO) chemical system using relevant activity–composition (*a–X*) models for melt, garnet, cordierite, staurolite, biotite, white mica, chlorite (White et al., 2014), orthoamphibole (Diener and Powell, 2011), ternary feldspar (Fuhrman and Lindsley, 1988), epidote (Holland and Powell, 2011), ilmenite (White et al., 2014) and magnetite (White et al., 2002). Pure phases included sillimanite, kyanite, andalusite, quartz, rutile and aqueous fluid (H_2O).

Compositional isopleths for garnet were calculated to further aid with the reconstruction of *P–T* paths. Detailed analytical conditions for the acquisition of whole-rock and garnet major element compositions, and information of the bulk-rock H_2O and ferric iron contents used for phase equilibrium modelling, are provided in the Supplementary

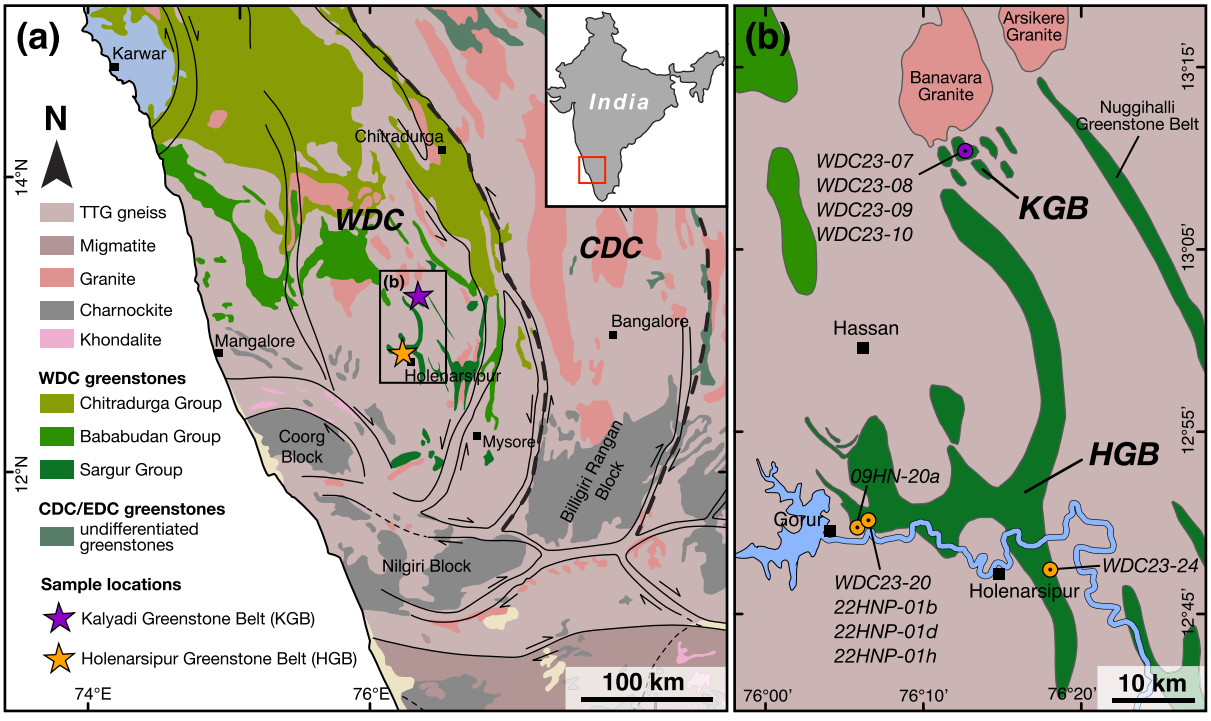

Fig. 1. (a) Simplified geological map of the Western Dharwar Craton (WDC) (modified after Ishwar-Kumar et al., 2013; Jayananda et al., 2023), and (b) close-up of the Kalyadi Greenstone Belt (KGB) and the Holenarsipur Greenstone Belt (HGB) in the core of the WDC showing the sample locations.

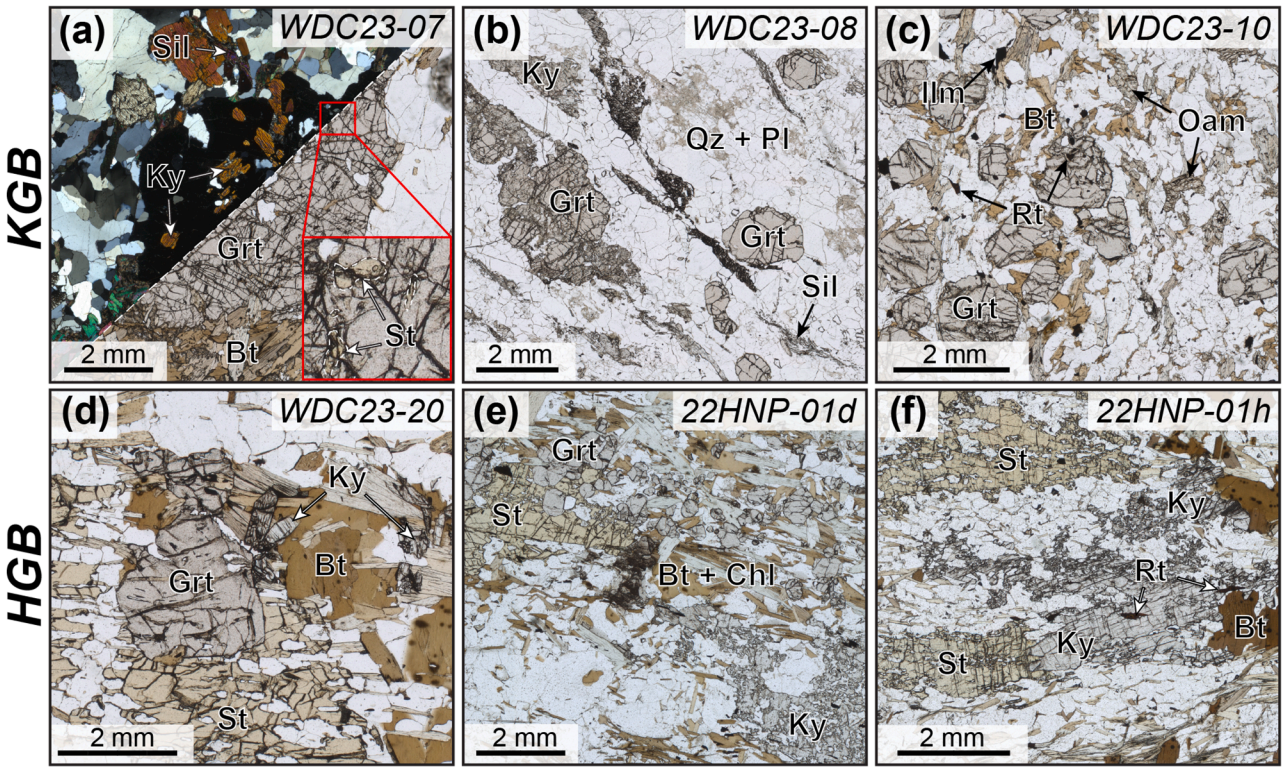

Fig. 2. Thin section photomicrographs showing representative mineral assemblages of samples from (a–c) the Kalyadi Greenstone Belt (KGB), and (d–f) the Holenarsipur Greenstone Belt (HGB). Grt–garnet; Ky–kyanite; Sil–sillimanite; St–staurolite; Oam–orthoamphibole; Bt–biotite; Chl–chlorite; Pl–plagioclase; Qz–quartz; Rt–rutile; Ilm–ilmenite.

Material S1.

3. Results

In situ LA–ICP–MS/MS of garnet from three metapelites (samples WDC23–07, 09, 10) and one peraluminous metatonalite (sample WDC23–08) from the KGB yielded isochron dates ranging from 2923 ± 65 Ma to 2975 ± 75 Ma, which define a single age population at 2962 ± 23 Ma (mean square of weighted deviates [MSWD] = 0.68, n = 4; Fig. 3a, c). Garnet from four metapelites from the HGB (samples WDC23–20, 09HN-20a, 22HNP-01b, d) returned distinctively younger Lu–Hf dates ranging from 2527 ± 16 Ma to 2543 ± 15 Ma, and constrain garnet growth in these rocks to 2538 ± 9 Ma (MSWD = 0.88, n = 4, Fig. 3b, c). The consistency of individual Lu–Hf isochron dates within their respective sample suite suggests that garnet growth in both the KGB and HGB was restricted to a single metamorphic event, albeit at different times (i.e., separated by ~400 Myr).

Monazite in metapelites from the KGB (samples WDC23–07, 09) typically occurs as rounded subhedral inclusions in garnet or as anhedral elongated grains in the matrix. Combining all analyses yields two clusters of concordant analyses, with evidence for partial Pb loss affecting some of the older grains (Fig. 4a). Concordant Mesoarchean analyses from monazite inclusions in garnet gave a weighted mean $^{207}Pb/^{206}Pb$ age of 2957 ± 7 Ma (MSWD = 0.89, n = 11; Fig. 4b). Monazite yielding concordant Neoarchean dates defines a weighted mean $^{207}Pb/^{206}Pb$ age of 2632 ± 12 Ma (MSWD = 3.5, n = 16), is typically associated with the matrix and has slightly lower Y concentrations and a less pronounced Eu anomaly ($Eu_N/Eu^*_N = Eu_N/(Sm_N{*}Gd_N)^{1/2}$) than Mesoarchean monazite (Fig. S3). By contrast, monazite in a garnet-absent schist from the HGB (sample WDC23–24) records a single concordant age population at 2491 ± 4 Ma (MSWD = 0.32, n = 32; Fig. 4c, d), with distinctively low Gd_N/Lu_N ratios and a weakly negative Eu anomaly (Fig. S3).

Phase equilibrium modelling of two garnet–orthoamphibole-bearing metapelites (samples WDC23–09, 10) and one garnet–kyanite-bearing metapelite from the KGB (sample WDC23–07) was employed to investigate the Mesoarchean metamorphic history (Fig. 5a–c). Whereas the inferred peak metamorphic assemblage of sample WDC23–07 was successfully reproduced using this approach, samples WDC23–09 and WDC23–10 were predicted to contain small amounts (< 2 vol. %) of kyanite in the inferred peak field, for which no evidence is preserved in the thin section. Nonetheless, the compositional isopleths for garnet rims in sample WDC23–10 suggest that these rocks did indeed equilibrate in the kyanite stability field (Fig. S5), which is in agreement with independent P–T estimates for kyanite-bearing sample WDC23–07. The intersection of the stability fields of the inferred mineral assemblages of all samples constrains peak metamorphic conditions to T = 685–700 °C and P = 10.9–11.3 kbar in the KGB (Fig. 6a). Constraints on the prograde metamorphic evolution were derived from growth-zoned garnet in sample WDC23–10, which displays a gradual compositional change from the core (X_{Mg} [= molar Mg/(Mg + Fe^{2+})] = 0.31, X_{Grs} [= molar Ca/(Ca + Mn + Mg + Fe^{2+})] = 0.09) to the rims (X_{Mg} = 0.38, X_{Grs} = 0.08) of porphyroblasts (Fig. S4), indicating a pressure increase and minor heating from ~665 °C and ~8.9 kbar to ~685 °C and ~10.5 kbar (Fig. S5). The inferred trajectory of the prograde P–T path for sample WDC23–10 is consistent with the prograde disappearance of staurolite in sample WDC23–07. Post-peak decompression to P < 7.5 kbar is inferred from the overgrowth of sillimanite on kyanite porphyroblasts in samples WDC23–07 and WDC23–08 (Fig. 2a, b) and the replacement of rutile by ilmenite.

Modelling of two garnet–staurolite–kyanite metapsammites (samples WDC23–20 and 22HNP-01d) and one staurolite–kyanite metapelite from the HGB (sample 22HNP-01 h) constrains Neoarchean peak conditions to T = 645–675 °C and P = 7.5–8.5 kbar (Figs. 5d–f; 6a). Nucleation and growth of garnet porphyroblasts in sample WDC23–20 is predicted to occur relatively early along the prograde path between ~450 °C at ~5.7 kbar (porphyroblast cores; X_{Mg} = 0.15, X_{Grs} = 0.14)

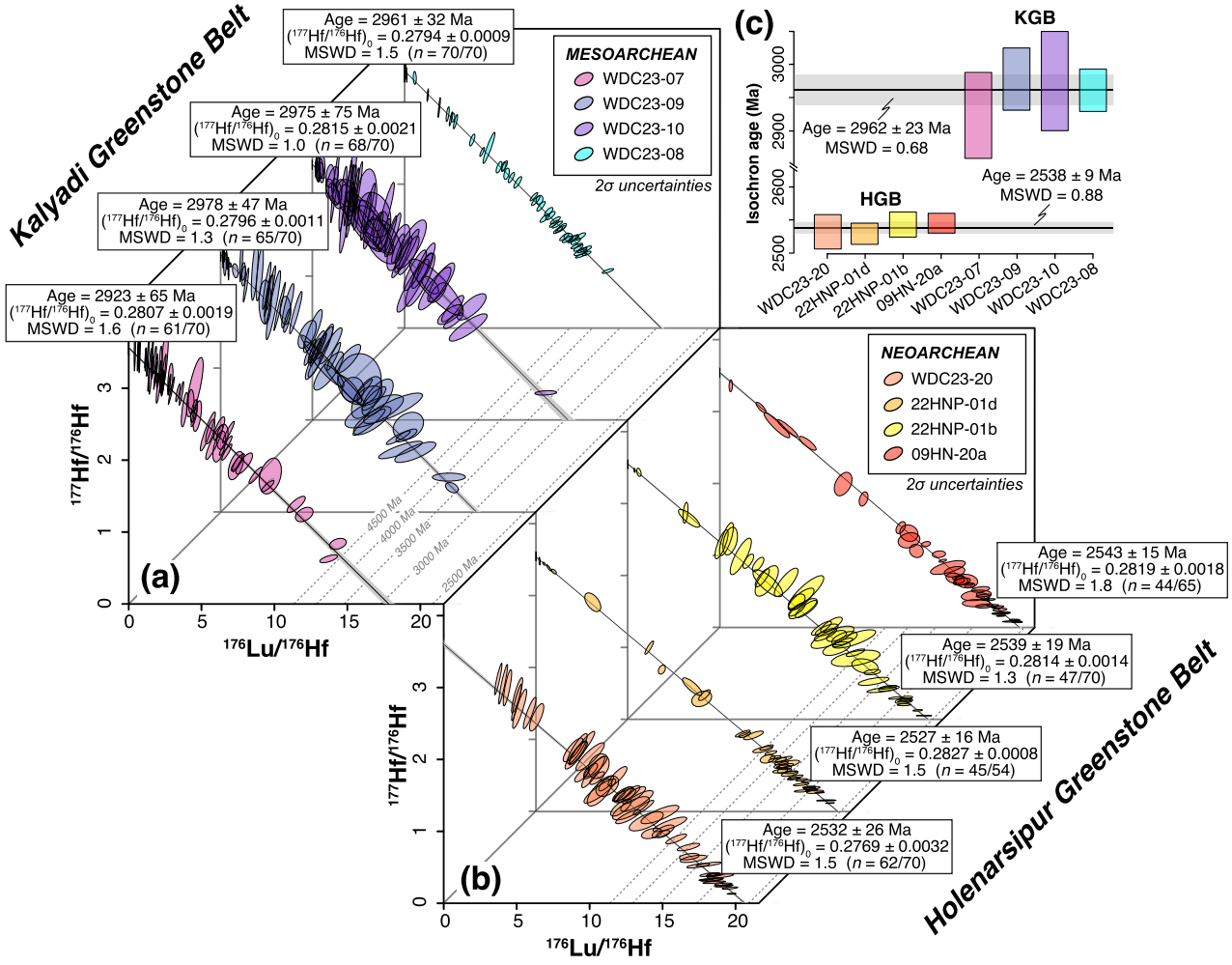

Fig. 3. Laser ablation–inductively coupled plasma–tandem mass spectrometry (LA–ICP–MS/MS) garnet Lu–Hf geochronology of representative samples from (a) the Kalyadi Greenstone Belt (KGB), and (b) the Holenarsipur Greenstone Belt (HGB). (c) Weighted mean ages for garnet growth in the KGB and HGB. MSWD–mean square of weighted deviates.

and ~520 °C at 7.2 kbar (porphyroblast rims and fine-grained garnet; $X_{Mg} = 0.17$, $X_{Grs} = 0.11$), and ceases completely thereafter during near-isobaric heating to peak conditions (Fig. S5). Early growth of garnet at pressures <6.5 kbar is further corroborated by the observation that porphyroblasts typically contain inclusions of ilmenite but lack rutile, the latter being the dominant matrix Fe–Ti oxide in sample WDC23–20. Petrographic observations and results from thermodynamic modelling are consistent with a clockwise *P–T* evolution for both Mesoarchean and Neoarchean metamorphism in the WDC.

4. Discussion

4.1. Limitations of our thermodynamic modelling in constraining the prograde metamorphic evolution

Our *P–T* estimates obtained for the prograde evolution of samples from the KGB and HGB rely on the assumption that the observed compositional zoning in garnet effectively reflects an unmodified record of the changing thermobaric conditions at which garnet grew. However, intracrystalline diffusion and/or re-equilibration of divalent cations during garnet growth and cooling are known to modify the compositional zoning of garnet at elevated temperatures, thereby affecting the *P–T* path estimates derived from them (e.g., Caddick et al., 2010; Florence and Spear, 1991; Spear, 1991). Our *P–T* estimates for the prograde metamorphic evolution of the two samples do not account for such syn-growth diffusional modifications of garnet, and may therefore potentially deviate from the 'true' *P–T* path they experienced. Nonetheless, we note that isopleths for the composition of garnet rims in sample WDC23–10, which we interpret to have grown at or close to the metamorphic peak, intersect within the inferred peak field of this sample (Fig. S5), suggesting that any post-growth diffusional overprinting was minor.

4.2. Garnet Lu–Hf dating reveals contrasting metamorphic histories in the WDC

In situ Lu–Hf dating of garnet reveals that supracrustal rocks from the KGB and HGB record two distinct metamorphic events in the Mesoarchean and Neoarchean, respectively. Whereas garnet growth in the HGB occurred at 2538 ± 9 Ma, garnet from the KGB yields an age of 2962 ± 23 Ma (Fig. 3). This age dichotomy is further reflected in the contrasting monazite age record of the two greenstone belts. Monazite in the HGB records a single metamorphic event at 2491 ± 4 Ma (Fig. 4d), in agreement with previous age estimates for Neoarchean metamorphism in the WDC (Bouhallier, 1995; Dasgupta et al., 2022; Jayananda et al., 2013), and most likely dates the final stages of microblock amalgamation within the Dharwar Craton (Jayananda et al., 2013; Li et al., 2018). Conversely, monazite inclusions in garnet from the KGB are of

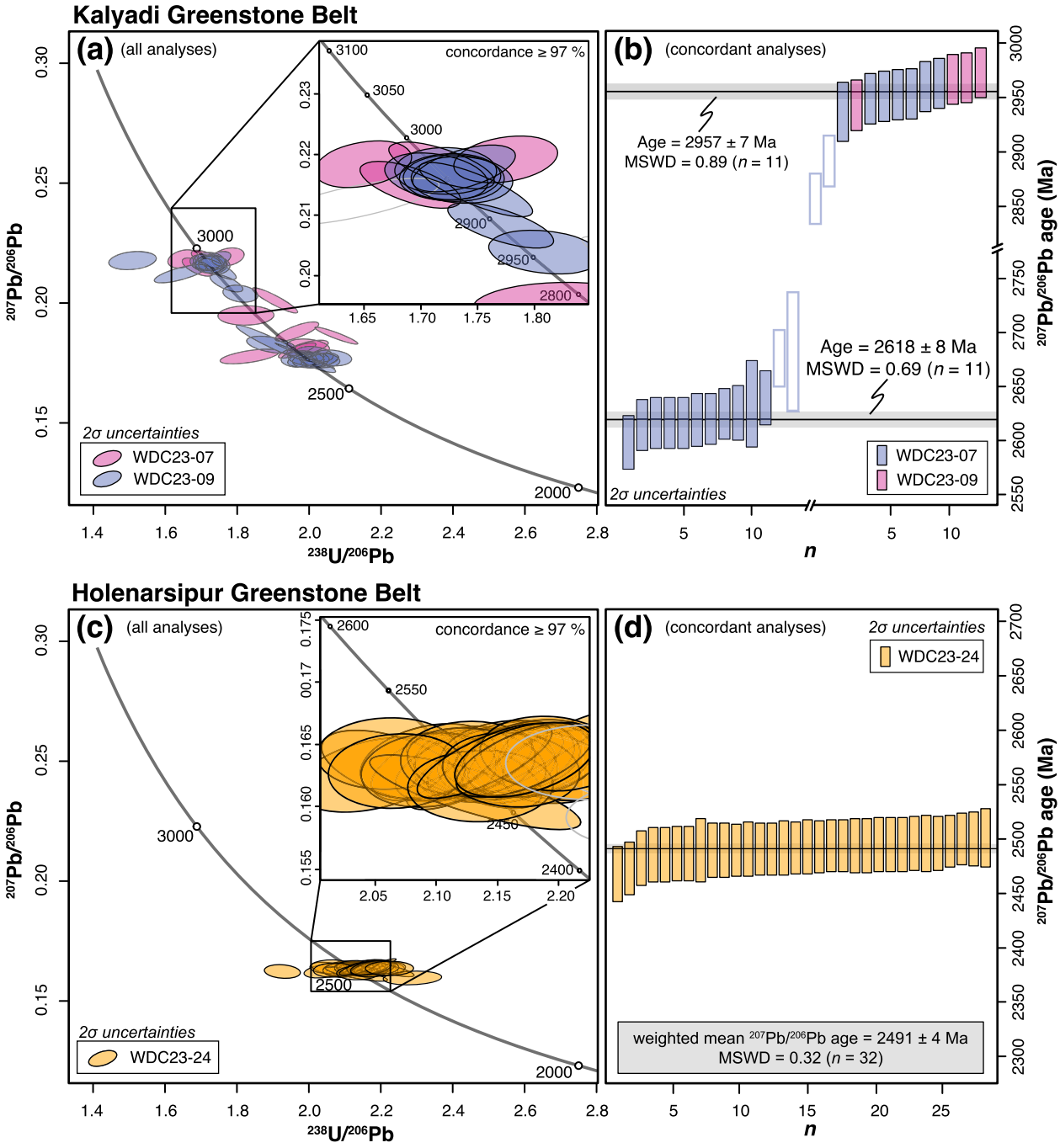

Fig. 4. Laser ablation–inductively coupled plasma–mass spectrometry (LA–ICP–MS) monazite U–Pb geochronology of representative samples from (a, b) the Kalyadi Greenstone Belt (KGB), and (c, d) the Holenarsipur Greenstone Belt (HGB). For the calculation of weighted mean $^{207}Pb/^{206}Pb$ ages, only those analyses which were ≥97 % concordant (defined here as the relative age difference between the $^{207}Pb/^{206}Pb$ and $^{238}U/^{206}Pb$ ages) within a given age cluster were considered. MSWD–mean square of weighted deviates.

Mesoarchean age (2957 ± 7 Ma; Fig. 4b), further supporting that the main metamorphic event recorded in the KGB occurred some 400 Myr earlier than in the HGB. Although previous findings of 3.14–3.10 Ga monazite in metapelitic samples from the central part of the HGB suggest that the belt experienced an earlier episode of Mesoarchean metamorphism (Dasgupta et al., 2019; Jayananda et al., 2013) some 180 million years before that in the KGB, we find no evidence for any pre-Neoarchean metamorphic event in our samples from the western and eastern parts of the HGB. Hence, we infer that the proportion of crust preserving evidence for this Mesoarchean event is small and restricted to low-strain domains that escaped widespread Neoarchean overprinting (Dasgupta et al., 2019). Based on these observations, and the apparent absence of a 2.54–2.49 Ga metamorphic overprint in samples from the KGB, we argue that the two greenstone belts experienced independent tectonothermal histories, at least until the late Neoarchean, as evidenced by *c.* 2.62 Ga monazite that occurs exclusively within the KGB (Fig. 4b).

The identification of Mesoarchean garnet in the KGB, coupled with thermobaric information preserved in the mineral assemblages of metapelitic rocks, reveals a previously unrecognized medium- to high-

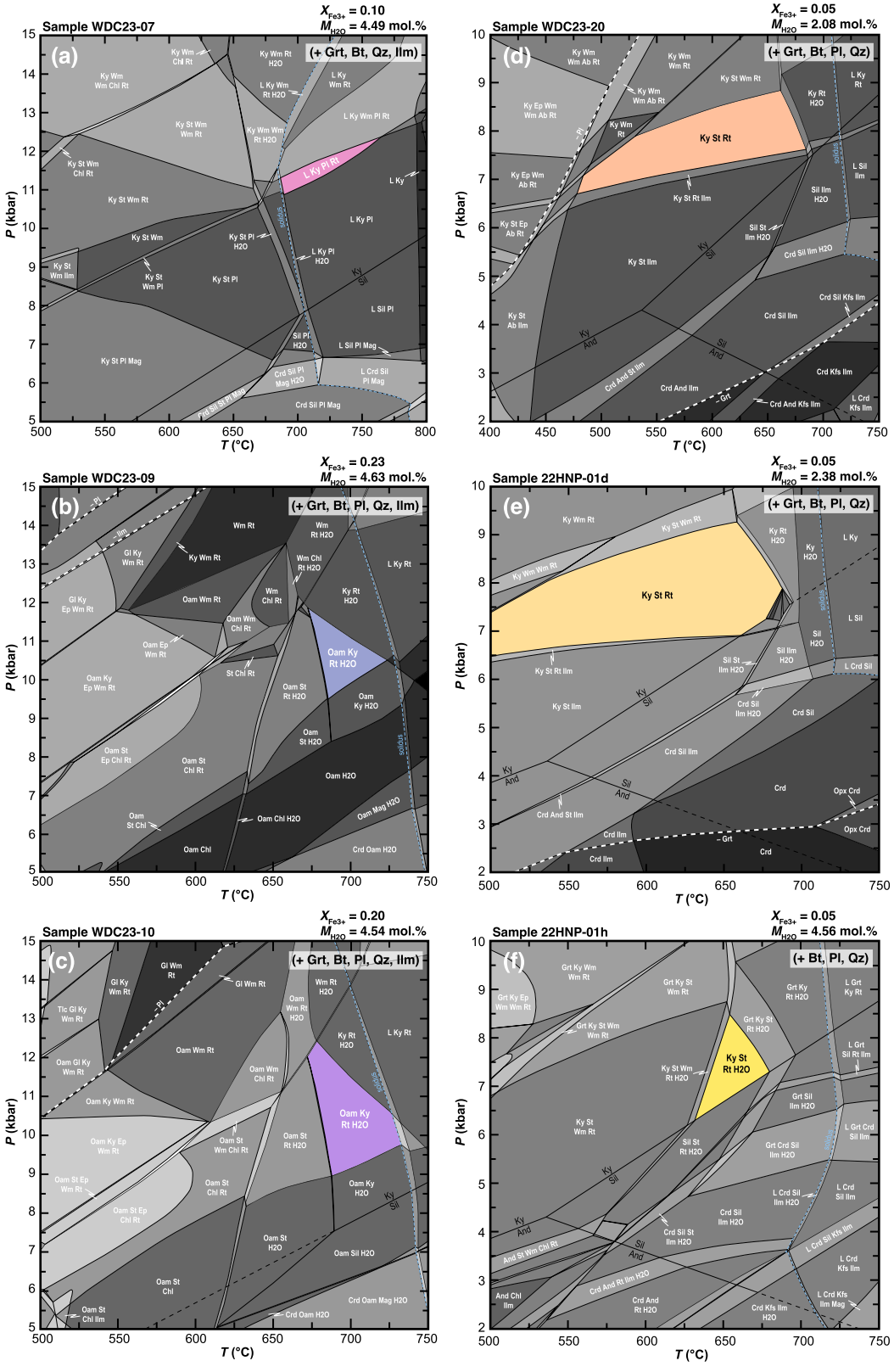

Fig. 5. Isochemical pressure–temperature (*P*–*T*) phase diagrams for low-variance samples from (a–c) the Kalyadi Greenstone Belt (KGB), and (d–f) the Holenarsipur Greenstone Belt (HGB). The inferred peak field for each sample is highlighted in color. L–melt; Grt–garnet; Ky–kyanite; Sil–sillimanite; And–andalusite; St–staurolite, Wm–white mica; Ep–epidote; Crd–cordierite; Opx–orthopyroxene; Oam–orthoamphibole; Bt–biotite; Chl–chlorite; Gl–glaucophane; Tlc–talc; Kfs–K-feldspar; Pl–plagioclase; Ab–albite; Qz–quartz; Rt–rutile; Ilm–ilmenite; Mag–magnetite.

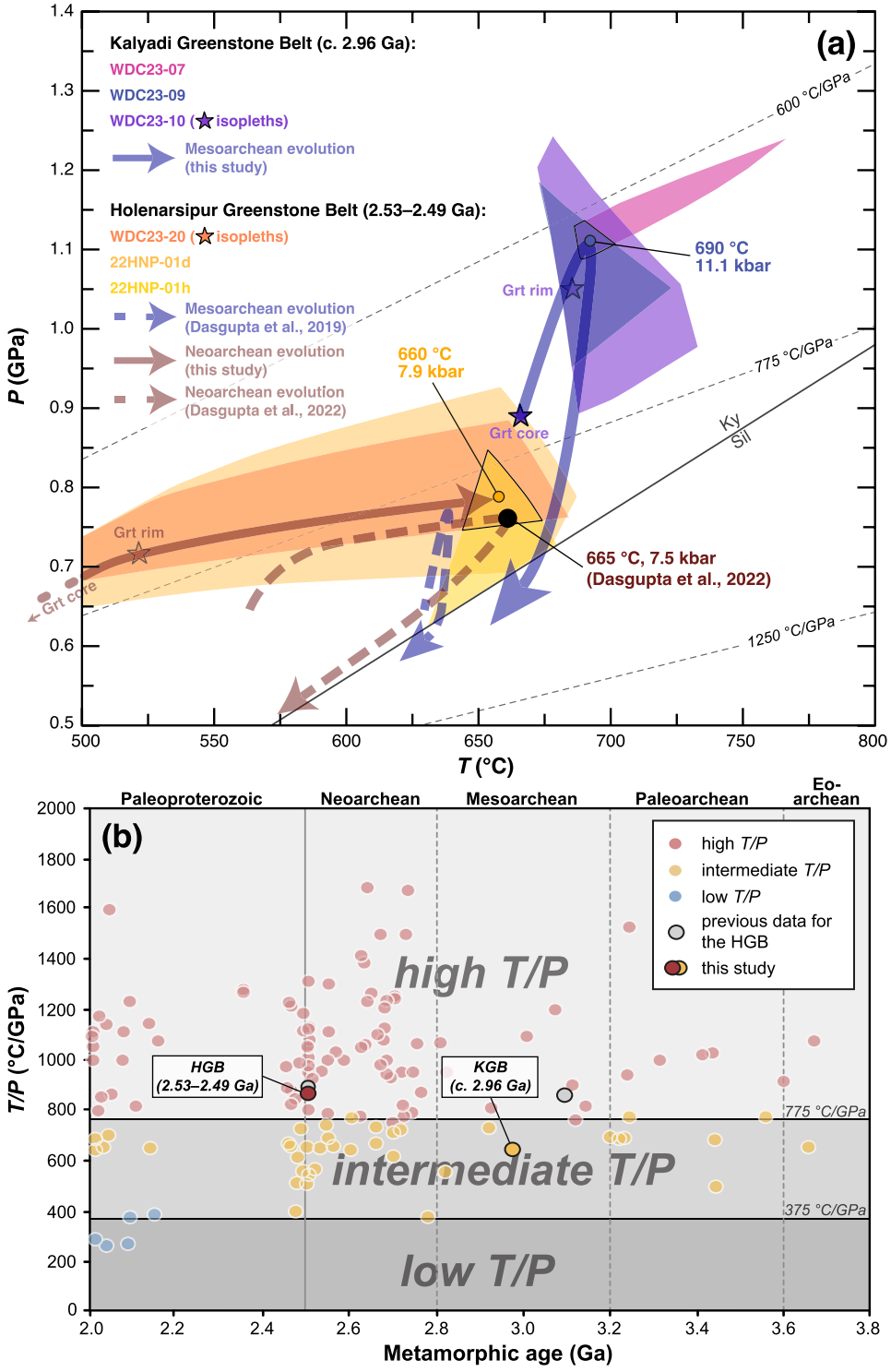

Fig. 6. (a) Pressure–temperature (*P–T*) diagram summarizing the thermobaric information preserved in metapelitic samples from the Kalyadi Greenstone Belt (KGB) and Holenarsipur Greenstone Belt (HGB). Existing constraints on the *P–T* evolution of the HGB (Dasgupta et al., 2019, 2022) and selected thermal gradients are shown for reference. (b) Comparison of peak metamorphic thermobaric ratios (*T/P*) of the KGB and HGB with other published data (reference data from Brown et al., 2024). Note the clear difference in the inferred thermobaric ratios for Mesoarchean metamorphism in the KGB (~630 °C/GPa) and the HGB (~860 °C/GPa).

pressure metamorphic event in the WDC. Despite the apparent mineralogical similarities of metapelites in the two greenstone belts, we demonstrate that Mesoarchean metamorphism in the KGB occurred at considerably higher pressures and slightly higher temperatures than Neoarchean metamorphism in the HGB (Fig. 6a). Notably, metapelitic rocks in the KGB record a thermobaric ratio (*T/P*) of ~630 °C/GPa during Mesoarchean (*c.* 2.96 Ga) peak metamorphism that is significantly lower (cooler) than existing estimates inferred for Mesoarchean metamorphism in the HGB (i.e., ~850 °C/GPa at *c.* 3.1 Ga; Dasgupta et al., 2019), suggesting that segments of Mesoarchean crust in the WDC,

which are now <50 km apart, evolved along contrasting thermal gradients.

The (partial) preservation of prograde compositional zoning in Mesoarchean garnet with seemingly undisturbed Lu–Hf systematics (Fig. 3a) requires that: (a) supracrustal rocks from the KGB resided for only a limited time at mid- to lower crustal depths (~40 km) before being exhumed, and (b) late growth of Neoarchean (*c.* 2.62 Ga) monazite, potentially facilitated in the presence of fluid (Williams et al., 2011), likely occurred at temperatures insufficient to induce extensive recrystallization of the Mesoarchean metamorphic assemblage. Our results highlight that, in the absence of additional temporal constraints from garnet, the age information recorded in monazite cannot unequivocally constrain the timing of the main (garnet-forming) metamorphic event, and may be prone to misinterpretation in complex polymetamorphic terranes.

4.3. A revised tectonothermal evolution for the Sargur Group

The age and thermobaric discrepancies between metapelites from the KGB and HGB reported herein demonstrate the shortcomings of current interpretations of a common tectonic evolution of Sargur Group supracrustal rocks in the WDC (Jayananda et al., 2013). Our findings, in combination with previous work (Dasgupta et al., 2019), suggest that the two neighboring greenstone belts underwent two temporally distinct metamorphic cycles, calling for a reassessment of the tectonothermal evolution of the Sargur Group.

Metamorphic ages of 2.96 Ga and 2.62 Ga recorded in the KGB closely overlap with the ages of potassic granite magmatism in the eastern WDC (Jayananda et al., 2018, 2006), but are otherwise absent from the temporal record in the WDC. Conspicuously, crustal reworking and associated high-grade metamorphism in the southern and western parts of the Central Dharwar Craton (CDC) have been constrained to 2.96 Ga and 2.62 Ga, respectively (Mahabaleswar et al., 1995; Mahabaleswar and Peucat, 1988; Nutman et al., 1992), postdating an even earlier tectono-metamorphic event at *c.* 3.2 Ga (Jayananda et al., 2011; Kaempf et al., 2024a). These observations suggest that Sargur Group greenstones in the eastern WDC, such as the KGB, may be more akin to stratigraphically equivalent greenstones in the western CDC than previously assumed. In this context, Barrovian-type medium- to high-pressure (~11 kbar) metamorphism at *c.* 2.96 Ga in the KGB, along with the occurrence of spatially-associated potassic granites, indicates that parts of the eastern WDC and western CDC record (at least) one episode of crustal thickening and partial melting at lower crustal levels that is not registered in other parts of the WDC (i.e., in the HGB), and vice versa. Such a scenario may be envisaged through continental collision of microblocks with distinct tectonothermal histories within the Dharwar Craton, possibly along regional subduction systems, prior to final amalgamation of the WDC and CDC in the late Neoarchean.

The absence of evidence for a late-Neoarchean metamorphic overprint affecting the KGB and other Sargur Group supracrustal rocks in the eastern WDC after 2.62 Ga (Hokada et al., 2013) is consistent with a lack of *c.* 2.5 Ga metamorphic ages reported from the central CDC, and insinuates that parts of the most ancient crust in the Dharwar Craton escaped extensive Neoarchean overprinting. Importantly, recognizing such ancient crustal remnants in other Archean cratons and establishing clear *P–T–t* relationships by integrating the temporal and thermobaric record of garnet will facilitate our efforts in retrieving robust constraints on crustal metamorphism during the first third of Earth's history – an endeavor that currently relies on <20 data points (Brown et al., 2024) but is of significant importance to understanding early Earth geodynamics more generally.

5. Conclusions

In situ Lu–Hf dating of garnet in metasedimentary rocks from the Western Dharwar Craton (WDC) coupled with monazite U–Pb dating and phase equilibrium modelling revealed contrasting metamorphic histories for two neighboring greenstone belts. While metapelitic rocks from the Holenarsipur Greenstone Belt (HGB) record Neoarchean (2.53–2.49 Ga) metamorphism (~8 kbar, ~660 °C) associated with final amalgamation of the craton, samples from the Kalyadi Greenstone Belt (KGB) preserve evidence for a Mesoarchean (2.96 Ga) medium- to high-pressure metamorphic event (~11 kbar, ~690 °C) that has previously not been recognized in the area. Our findings show that the *P–T–t* records of supracrustal rocks in the WDC are inconsistent with a common tectonothermal evolution, but instead require separate histories for these greenstone belts throughout the Mesoarchean and Neoarchean. The temporal record of metamorphism and associated crustal recycling in the KGB aligns more closely with the evolution of greenstones exposed in the western and southern parts of the Central Dharwar Craton (CDC).

CRediT authorship contribution statement

Jonas Kaempf: Visualization, Investigation, Conceptualization, Writing – original draft. **Chris Clark:** Writing – review & editing, Conceptualization. **Tim E. Johnson:** Writing – review & editing, Conceptualization. **Mudlappa Jayananda:** Writing – review & editing, Resources. **Martin Hand:** Writing – review & editing, Investigation. **Krishnan Sajeev:** Writing – review & editing, Resources.

Declaration of competing interest

The authors declare that they have no known competing financial interests or personal relationships that could have appeared to influence the work reported in this paper.

Acknowledgements

This research was supported by Australian Research Council (ARC) grant DP200101104 to TEJ and CC. MJ is supported by J.C. Bose National Fellowship grant for fieldwork and sample processing. We thank J. Alfing and K.R. Aadhiseshan for support during fieldwork and sample processing, and K. Rankenburg for discussions. Constructive comments by Fred Gaidies and an anonymous reviewer are gratefully acknowledged.

Supplementary materials

Supplementary material associated with this article can be found, in the online version, at doi:10.1016/j.epsl.2025.119545.

Data availability

The data that support the findings of this study are available in the supplementary materials of this article (S1–S2).

References

Alfing, J., Johnson, T.E., Kaempf, J., Brown, M., Szilas, K., Rankenburg, K., Clark, C., 2024. Eoarchean granulite-facies metamorphism in the Itsaq Gneiss complex, southwest Greenland. Earth Planet. Sci. Lett. 646, 118977. https://doi.org/10.1016/j.epsl.2024.118977.

Baxter, E.F., Caddick, M.J., Dragovic, B., 2017. Garnet: a rock-forming mineral petrochronometer. Rev. Mineral. Geochem. 83, 469–533. https://doi.org/10.2138/rmg.2017.83.15.

Bouhallier, H., 1995. Evolution Structurale Et Métamorphique De La Croûte Continentale Archéenne (craton de Dharwar, Inde du Sud). Mémoires de Géosciences. Géosciences, Université de Rennes I, Rennes.

Brown, M., Johnson, T., 2018. Secular change in metamorphism and the onset of global plate tectonics. Am. Mineral. 103, 181–196. https://doi.org/10.2138/am-2018-6166.

Brown, M., Pearce, J.A., Johnson, T.E., 2024. Is plate tectonics a post-Archean phenomenon? A petrological perspective. J. Geol. Soc. Lond. 181, jgs2024–jgs2091. https://doi.org/10.1144/jgs2024-091.

Caddick, M.J., Konopásek, J., Thompson, A.B., 2010. Preservation of garnet growth zoning and the duration of prograde metamorphism. J. Petrol. 51, 2327–2347. https://doi.org/10.1093/petrology/egq059.
Connolly, J., 1990. Multivariable phase diagrams: an algorithm based on generalized thermodynamics. Am. J. Sci. 290, 666–718. https://doi.org/10.2475/ajs.290.6.666.
Connolly, J.a.D., 2009. The geodynamic equation of state: what and how. Geochem. Geophys. Geosyst. 10. https://doi.org/10.1029/2009GC002540.
Connolly, J.A.D., 2005. Computation of phase equilibria by linear programming: a tool for geodynamic modeling and its application to subduction zone decarbonation. Earth Planet. Sci. Lett. 236, 524–541. https://doi.org/10.1016/j.epsl.2005.04.033.
Cutts, K.A., Lana, C., Stevens, G., Buick, I.S., 2024. In situ Pb–Pb garnet geochronology as a tool for investigating polymetamorphism: a case for Paleoarchean lateral tectonic thickening. Spec. Publ. 537, 209–229. https://doi.org/10.1144/SP537-2022-339.
Dasgupta, A., Bhowmik, S.K., Dasgupta, S., 2022. Transition in thermal history and recurring burial-exhumation cycles along colder thermal gradients at the archaean-Proterozoic boundary: new insights from the Western Dharwar Craton, South India. J. Petrol. 63, egac041. https://doi.org/10.1093/petrology/egac041.
Dasgupta, A., Bhowmik, S.K., Dasgupta, S., Avila, J., Ireland, T.R., 2019. Mesoarchaean clockwise metamorphic P-T path from the Western Dharwar Craton. Lithos 342–343, 370–390. https://doi.org/10.1016/j.lithos.2019.06.006.
Diener, J.F.A., Powell, R., 2011. Revised activity–composition models for clinopyroxene and amphibole. J. Metamorph. Geol. 30, 131–142. https://doi.org/10.1111/j.1525-1314.2011.00959.x.
Florence, F.P., Spear, F.S., 1991. Effects of diffusional modification of garnet growth zoning on P-T path calculations. Contr. Mineral. Petrol. 107, 487–500. https://doi.org/10.1007/BF00310683.
Fuhrman, M.L., Lindsley, D.H., 1988. Ternary-feldspar modeling and thermometry. Am. Mineral. 73, 201–215.
Hermann, J., Rubatto, D., 2003. Relating zircon and monazite domains to garnet growth zones: age and duration of granulite facies metamorphism in the Val Malenco lower crust. J. Metamorph. Geol. 21, 833–852. https://doi.org/10.1046/j.1525-1314.2003.00484.x.
Hokada, T., Horie, K., Satish-Kumar, M., Ueno, Y., Nasheeth, A., Mishima, K., Shiraishi, K., 2013. An appraisal of Archaean supracrustal sequences in Chitradurga Schist Belt, Western Dharwar Craton, Southern India. Precambrian Res. 227, 99–119. https://doi.org/10.1016/j.precamres.2012.04.006.
Holland, T.J.B., Powell, R., 2011. An improved and extended internally consistent thermodynamic dataset for phases of petrological interest, involving a new equation of state for solids. J. Metamorph. Geol. 29, 333–383. https://doi.org/10.1111/j.1525-1314.2010.00923.x.
Jayananda, M., Banerjee, M., Pant, N.C., Dasgupta, S., Kano, T., Mahesha, N., Mahabaleswar, B., 2011. 2.62 Ga high-temperature metamorphism in the central part of the Eastern Dharwar Craton: implications for late Archaean tectonothermal history. Geol. J. 47, 213–236. https://doi.org/10.1002/gj.1308.
Jayananda, M., Chardon, D., Peucat, J.J., Capdevila, R., 2006. 2.61Ga potassic granites and crustal reworking in the western Dharwar craton, southern India: tectonic, geochronologic and geochemical constraints. Precambrian Res. 150, 1–26. https://doi.org/10.1016/j.precamres.2006.05.004.
Jayananda, M., Guitreau, M., Aadhiseshan, K.R., Miyazaki, T., Chung, S.L., 2023. Origin of the oldest (3600–3200 Ma) cratonic core in the Western Dharwar Craton, Southern India: implications for evolving tectonics of the Archean Earth. Earth Sci. Rev. 236, 104278. https://doi.org/10.1016/j.earscirev.2022.104278.
Jayananda, M., Kano, T., Peucat, J., Channabasappa, S., 2008. 3.35Ga komatiite volcanism in the western Dharwar craton, southern India: constraints from Nd isotopes and whole-rock geochemistry. Precambrian Res. 162, 160–179. https://doi.org/10.1016/j.precamres.2007.07.010.
Jayananda, M., Tsutsumi, Y., Miyazaki, T., Gireesh, R.V., Kapfo, K., Tushipokla, Hidaka, H., Kano, T., 2013. Geochronological constraints on Meso- and Neoarchean regional metamorphism and magmatism in the Dharwar craton, southern India. J. Asian Earth Sci. 78, 18–38. https://doi.org/10.1016/j.jseaes.2013.04.033.
Jayananda, Santosh, Aadhiseshan, 2018. Formation of Archean (3600–2500 Ma) continental crust in the Dharwar Craton, southern India. Earth Sci. Rev. 181, 12–42. https://doi.org/10.1016/j.earscirev.2018.03.013.
Kaempf, J., Clark, C., Johnson, T.E., Jayananda, M., Alfing, J., Payne, J., Sajeev, K., Hand, M., 2024a. Archean Polymetamorphism in the Central Dharwar Craton, Southern India. J. Metamorph. Geol. 43, 71–95. https://doi.org/10.1111/jmg.12798.
Kaempf, J., Johnson, T.E., Clark, C., Alfing, J., Brown, M., Lanari, P., Rankenburg, K., 2024b. Paleoarchean metamorphism in the Acasta Gneiss Complex: constraints from phase equilibrium modelling and in situ garnet Lu–Hf geochronology. J. Metamorph. Geol. 42, 373–394. https://doi.org/10.1111/jmg.12759.
Kuang, J., Morra, G., Yuen, D.A., Kusky, T., Jiang, S., Yao, H., Qi, S., 2023. Metamorphic constraints on Archean tectonics. Precambrian Res. 397, 107195. https://doi.org/10.1016/j.precamres.2023.107195.
Li, S.S., Santosh, M., Palin, R.M., 2018. Metamorphism during the Archean–Paleoproterozoic Transition Associated with Microblock Amalgamation in the Dharwar Craton, India. J. Petrol. 59, 2435–2462. https://doi.org/10.1093/petrology/egy102.
Mahabaleswar, B., Jayananda, M., Peucat, J.J., Swamy, N., 1995. Archaean high-grade gneiss complex from Satnur-Halagur-Sivasamudram areas, Karnataka, southern India: petrogenesis and crustal evolution. J. Geol. Soc. India 45, 33–49.
Mahabaleswar, B., Peucat, J.J., 1988. 2.9 by. Rb-Sr age of the granulite facies rocks of Satnur-Halagur and Sivasamudram Areas, Karnataka, South India. J. Geol. Soc. India 32, 461–467.
Nutman, A.P., Chadwick, B., Ramakrishnan, M., Viswanatha, M.N., 1992. Shrimp U-Pb Ages of Detrital Zircon in Sargur Supracrustal Rocks in Western Karnataka, Southern India. J. Geol. Soc. India 39, 367–374.
Palin, R.M., Santosh, M., Cao, W., Li, S.S., Hernández-Uribe, D., Parsons, A., 2020. Secular change and the onset of plate tectonics on Earth. Earth Sci. Rev. 207, 103172. https://doi.org/10.1016/j.earscirev.2020.103172.
Simmat, R., Raith, M., 2008. U–Th–Pb monazite geochronometry of the Eastern Ghats Belt, India: timing and spatial disposition of poly-metamorphism. Precambrian Res. 162, 16–39. https://doi.org/10.1016/j.precamres.2007.07.016.
Simpson, A., Gilbert, S., Tamblyn, R., Hand, M., Spandler, C., Gillespie, J., Nixon, A., Glorie, S., 2021. In-situ LuHf geochronology of garnet, apatite and xenotime by LA ICP MS/MS. Chem. Geol. 577, 120299. https://doi.org/10.1016/j.chemgeo.2021.120299.
Skublov, S.G., Astaf'ev, B.Yu., Marin, Yu.B., Berezin, A.V., Mel'nik, A.E., Presnyakov, S. L., 2011. New data on the age of eclogites from the Belomorian mobile belt at Gridino settlement area. Dokl. Earth Sci. 439, 1163–1170. https://doi.org/10.1134/S1028334X11080290.
Spear, F.S., 1991. On the interpretation of peak metamorphic temperatures in light of garnet diffusion during cooling. J. Metamorph. Geol. 9, 379–388. https://doi.org/10.1111/j.1525-1314.1991.tb00533.x.
Volodichev, O.I., Maksimov, O.A., Kuzenko, T.I., Slabunov, A.I., 2021. Archean zircons with omphacite inclusions from Eclogites of the Belomorian province, Fennoscandian shield: the first finding. Minerals 11, 1029. https://doi.org/10.3390/min11101029.
White, R.W., Powell, R., Clarke, G.L., 2002. The interpretation of reaction textures in Fe-rich metapelitic granulites of the Musgrave Block, central Australia: constraints from mineral equilibria calculations in the system K2O–FeO–MgO–Al2O3–SiO2–H2O–TiO2–Fe2O3. J. Metamorph. Geol. 20, 41–55. https://doi.org/10.1046/j.0263-4929.2001.00349.x.
White, R.W., Powell, R., Holland, T.J.B., Johnson, T.E., Green, E.C.R., 2014. New mineral activity–composition relations for thermodynamic calculations in metapelitic systems. J. Metamorph. Geol. 32, 261–286. https://doi.org/10.1111/jmg.12071.
Williams, M.L., Jercinovic, M.J., Harlov, D.E., Budzyń, B., Hetherington, C.J., 2011. Resetting monazite ages during fluid-related alteration. Chem. Geol. 283, 218–225. https://doi.org/10.1016/j.chemgeo.2011.01.019.